19 July 1996

ELSEVIER

Chemical Physics Letters 257 (1996) 49–60

CHEMICAL PHYSICS LETTERS

Relative stability of $^1C_4$ and $^4C_1$ chair forms of β-D-glucose: a density functional study

Gábor I. Csonka [a], Krisztina Éliás [a], Imre G. Csizmadia [b]

[a] *Department of Inorganic Chemistry, Technical University of Budapest, H-1521 Budapest, Hungary*
[b] *Department of Chemistry, University of Toronto, Toronto, Ontario, Canada M5S 1A1*

Received 14 March 1996; in final form 26 April 1996

Abstract

The method and basis set dependence of the relative energies of the $^1C_4$ and $^4C_1$ chair forms of β-D-glucose were calculated for two selected, low-energy hydroxyl rotamers at various levels of generalized gradient approximation density functional theory (GGA-DFT). The GGA-DFT and MP2 methods provide similar energetic differences for β-D-glucose conformers. Addition of the diffuse functions to a double-zeta quality basis set and inclusion of the HF exchange into the DFT functionals improve the agreement between the DFT and the best composite estimates of the energetic differences. The GGA- or hybrid-DFT methods reproduce the geometrical consequences of correlation effects correctly for glucose.

1. Introduction

Because of its biochemical importance D-glucose has been the subject of a series of recent theoretical studies [1–10]. These studies address questions related to the stability of hydroxyl and hydroxymethyl rotamers, the ring conformation, the structural and energetic consequences of anomeric effect, and solvation effects. Recent studies show a considerable agreement for the anomeric and solvation effects [3,4,6–8,11], providing that the differential anomeric solvation effect is less than 1 kcal/mol.

Polavarapu and Ewig [4], as well as Schleyer and Salzner [8] showed for the hydroxymethyl rotamers of D-glucose, at HF/4-31G and 6-31G(d) levels of theory, respectively, that the rotation of the exocyclic hydroxymethyl group has no influence on the energy difference between the α and β anomers. The three-fold rotation of the four hydroxyl and the hydroxymethyl groups, in principle, can generate $3^\circ = 729$ different rotamers. Fig. 1 shows several rotamers of the $^4C_1$ and $^1C_4$ conformers of β-D-glucose using the notations of our previous paper [12]. Note that only the carbon atoms are numbered. These same numbers will be used to denote the oxygen atoms attached to those carbons throughout the paper. The idealized dihedral angles of the $C(n+1)$–$C(n)$–$O(n)$–H torsions, where $n = 1, 2, 3, 4$ are designated by g+, t and g− for gauche clockwise (60°), anti (180°) and gauche counterclockwise (−60°), respectively. The idealized O5–C5–C6–O6 dihedral angles for the hydroxymethyl group are denoted by capital letters (G+, T and G− as shown in Fig. 1).

NMR results for the rotamers of the hydroxymethyl group in the $^4C_1$ conformer of D-glucose provided that the G− and G+ rotamers were populated in about 55:45 ratio at room temperature,

PII S0009-2614(96)00508-8

while the population of the T rotamer was negligible (less than 2%) [13]. In the crystal structure of α-D-glucose [14] the G − orientation was found for the hydroxymethyl group. However, the crystal structure represents a conformer of considerably higher energy, by 8 kcal/mol at the HF/6-31G(d) level of theory, because in this geometry the unfavorable orientations of the OH groups decrease the number of intramolecular hydrogen bridges [8]. At the HF/6-31G(d) level of theory the G − g + hydroxymethyl rotamer is the most stable, however, the differences between the three rotamers are below 0.2 kcal/mol [12]. At the HF/4-31G level of theory the T rotamer is the most stable [4]. The inclusion of the Gibbs energy corrections stabilizes the G − rotamer, however, it becomes only slightly more stable (by 0.02 kcal/mol [4]) than the T rotamer. Barrows et al. [10] have shown that a large (cc-pVTZ or larger) basis set is required to get the correct energetic order for the hydroxymethyl rotamers at the MP2 level of theory. Basis set extension corrections (up to cc-pV^{T}QZ basis set) and correlation corrections (up to CCSD level) were also proposed.

The conformation of the aldopyranosyl ring is also an important issue. For β-D-glucopyranose it is well known that it takes an all-equatorial chair conformation, designated $^4C_1$ in Fig. 1. An alternative chair conformation, designated $^1C_4$ in Fig. 1, puts all substituents in axial positions. Beside the correct description of various rotamers, the accurate modeling of the energetic and structural consequences of aldopyranose ring puckering is a challenging task even for the most advanced levels of theory. The results of Barrows et al. [10] show again that only expensive MP2 calculations are able to reproduce the experimental energetic order. However, such calculations are clearly too demanding to become routine on a series of rotamers or conformers, or for larger oligosaccharides.

The primary focus of this Letter is to find an economical alternative which can provide reliable energetic order and molecular geometry for glucopyranoses. These methods will be tested on further series of various hexapyranoses. The results of Barrows et al. [10] will be used as a benchmark in this Letter, thus we follow the selection of Barrows et al. [10]. The following codes identify the four selected conformers (see Fig. 1): **(1)** $^4C_1$ [t t t t G + g −], **(2)** $^4C_1$ [t t t t T g +], **(3)** $^1C_4$ [t g + g − − g − G + g +], **(4)** $^1C_4$ [g − − g + + g − − g + + G − g −], where the order of the code letters follows the clockwise sequential numbers of the carbon atoms in

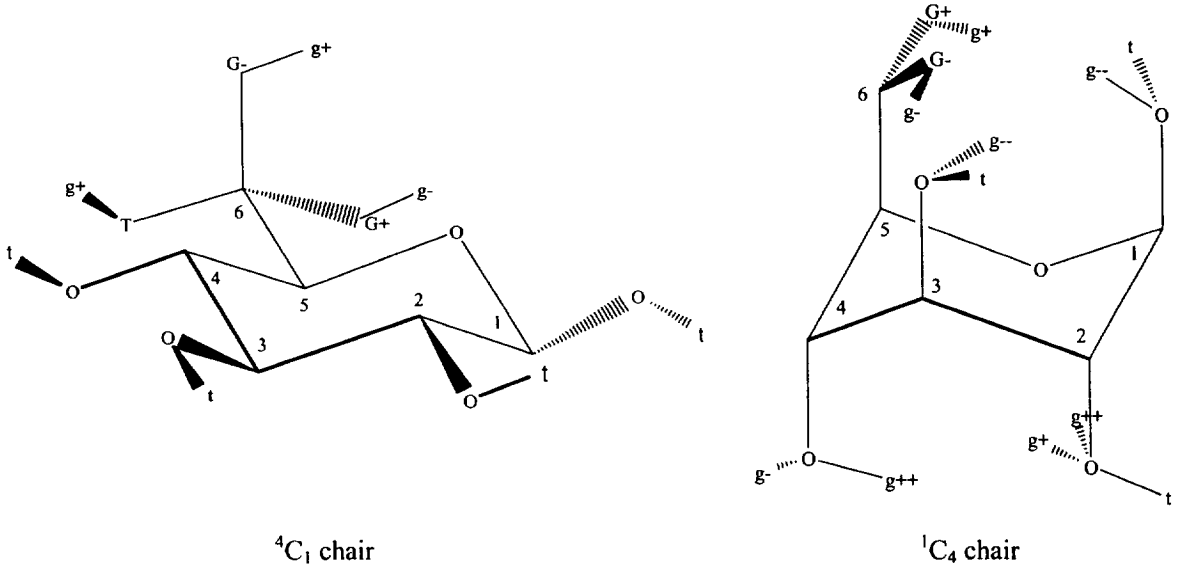

$^4C_1$ chair $^1C_4$ chair

Fig. 1. Schematic representation of some $^1C_4$ and $^4C_1$ chair hydroxyl and hydroxymethyl rotamers of β-D-glucose. The idealized C(n + 1)–C(n)–O–H torsions are denoted by g + , t and g − for gauche clockwise (60°), anti (180°) and gauche counterclockwise (−60°) respectively, where n = 1, 2, 3, 4. The idealized O5–C5–C6–O6 dihedral angles for the hydroxymethyl group are denoted by capital letters: G + , T and G − , g + + or g − − notate torsions far from the idealized values for the $^1C_4$ chair conformer.

Fig. 1, and g + + or g − − denotes further deviation compared to the idealized angles.

It should be noted that the selection of the conformers by Barrows et al. [10] is somewhat arbitrary. For example, the $^4C_1$ [t t t t G − g +] conformation, which was not considered, is certainly close in energy to conformers (1) and (2). It is also possible that other rotamers may be equally or more stable than conformers (3) and (4). However, our results show that some of the important features of the conformational space is well represented by these four conformers and they are suitable for benchmark purposes. The analysis of these structures leads to a better understanding of the real features of aldohexapyranose rings and the role of the electron correlation effects in the OH · · · O interactions.

2. Computational methods

We use the following combinations of the DFT functionals:

(i) BP or Becke–Perdew method, in which Becke's exchange functional [15] is combined with Perdew's correlation functional [16].

(ii) B3P is a hybrid method. It is a three-parameter linear combination of the HF, Slater and Becke exchange functionals, and Vosko, Wilk and Nusair [17] and Perdew [16] correlation functionals. The parameters A, B and C were determined by Becke by fitting heats of formations ($A = 0.2$, $B = 0.72$, $C = 0.81$) [18]. Note that Becke used the Perdew–Wang (PW91) functional instead of P86 [18].

(iii) B3LYP is a hybrid method. This functional was first implemented into the GAUSSIAN 92/DFT [19] program. It is a logical extension of Becke's three-parameter concept using the LYP correlational functional [20].

The geometries were optimized using the Berny algorithm combined with redundant internal coordinates built into the GAUSSIAN 94 program [21]. The DFT calculations were carried out using the sg1 (pruned to about 3000 points per atom) and fine

Table 1
Calculated total (E_h) and relative (kcal/mol) energies of the four selected β-D-glucose conformers [a]

Method	Conformer			
	(1)	(2)	(3)	(4)
HF/3-21G	−679.55250	−2.09	−6.55	−7.68
HF/6-31G(d)	−683.33194	−0.15	6.73	6.76
HF/cc-pVDZ [b]	−683.40610	−0.09	6.23	6.34
HF/cc-pVTZ//HF/cc-pVDZ [b]	−683.61764	0.35	9.78	9.87
HF/cc-pTVQZ//MP2/cc-pVDZ [b]	−683.65029	0.48	13.07	16.78
MP2/6-31G(d) [b]	−685.17603	−0.45	0.66	−0.60
MP2/cc-pVDZ [b]	−685.34107	−0.50	−0.11	−0.81
CCSD/6-31G(d)//MP2/6-31G(d) [b]	−685.24789	−0.34	2.07	1.68
MP2/cc-pVTZ//MP2/cc-pVDZ [b]	−686.05046	0.07	4.13	3.65
composite E [b]	−686.16144	0.27	6.41	6.99
composite G_{298} (rot-vib) [b]	−685.97132	0.58	8.24	8.80
BP/6-31G(d)	−687.15320	−0.77	−0.66	−4.40
B3P/cc-PVDZ//MP2/cc-pVDZ	−688.94839	−0.89	−0.16	−2.45
B3LYP/6-31G(d)	−687.14920	−0.70	1.65	−0.60
B3P/6-311G(d,p)//MP2/cc-pVDZ	−689.09736	−0.52	2.15	0.85
B3P/6-31G(d)	−688.88034	−0.80	2.97	
BP/6-31 + G(d)//MP2/cc-pVDZ	−687.19506	−0.16	3.39	1.69
BP/6-31 + G(d)	−687.19818	−0.15	4.94	2.79
B3P/6-31 + G(d)//MP2/cc-pVDZ	−688.91578	−0.30	5.43	4.24
B3P/aug-cc-PVDZ//MP2/cc-pVDZ	−689.02121	0.02	6.18	5.28
B3LYP/6-31 + G(d)	−687.19449	−0.12	6.92	4.93
B3LYP/6-31 + G(d)//MP2/cc-pVDZ	−687.19207	−0.16	7.19	6.74

[a] See text for the numbering and geometry of conformers.
[b] Ref. [10].

(pruned to about 7000 points per atom) grids. The 6-31G(d), 6-31 + G(d), 6-311G(d,p) [22], cc-pVDZ, and aug-cc-pVDZ [23] basis sets were used. The calculations were performed on Silicon Graphics and IBM workstations.

3. Results and discussion

3.1. Relative energies

Earlier results, in Table 1, show that there is a monotonic change in the energetic order as the basis set quality increases at the HF level of theory. The HF/3-21G results are inadequate for the energetic order because the HF/3-21G method overstabilizes the $^1C_4$ conformers relative to the $^4C_1$ conformers. The HF/6-31G(d) and cc-pVDZ results provide quite good relative energies that are close to the results of the most expensive calculations, while the HF/cc-pVTZ or cc-pV^{T}QZ methods understabilize the $^1C_4$ conformers [10]. The HF method supplemented with good quality basis sets tends to underestimate the H · · · OH interactions, because it overconcentrates the electron density around the atoms and in the normal covalent bonding regions and underconcentrates it in the other regions of space. The $^1C_4$ conformations are sensitive to this effect because the strength of the 1–3 OH interactions may easily be decreased by small (low-energy) deformations of the $^1C_4$ ring and the exocyclic hydroxyl groups causing considerable increase in the H · · · O distances. The monotonic change in the relative stabilities as a function of basis set quality provides an opportunity to find a basis set for which the basis set truncation error compensates the inherent deficiencies of the HF method for the relative energies of the four conformers studied in this Letter. Using a double-zeta quality basis set is close to the optimal choice for this type of energetic order at the HF level of theory (see Table 1).

The results of Barrows et al. [10] show that the inclusion of the electron correlation at the MP2, CCSD/6-31G(d) and MP2/cc-pVDZ levels of theory provide rather poor energetic order (Table 1). This is expected because the introduction of electron correlation increases the H · · · OH stabilization effects for the $^1C_4$ ring relative to the HF method, thus worsening the good HF results by 6–7 kcal/mol. Considerably larger basis sets (cc-pVTZ or larger, see Table 1) are required at the MP2 level of theory to approach the real energetic order somewhat better. It should be noted that even this level of theory is not fully satisfactory and further basis set and correlation corrections are necessary to improve the results [10]. This behavior limits the applicability and value of MP2 calculations for conformational studies of aldohexapyranoses. It should be noted that the computational expense of the MP2 method is formally $O(N^5)$, where N is the number of basis functions in the molecule. The DFT methods may provide a less expensive alternative for estimating correlation effects. The cost is formally $O(N^3)$, which may be reduced by efficient implementations [24].

The results in Table 1 show that the various DFT methods supplemented with the double-zeta quality basis set provide similar energetic results as the MP2 method. They fail in the same way as the MP2 method failed. However, the results also show that the addition of diffuse functions (e.g. 6-31 + G(d) or aug-cc-pVDZ) improve considerably the DFT energetic order. This is because the diffuse functions provide a space for the electrons far from the nuclei, thus the long-range part of the correlation and exchange functionals work better for the OH · · · O interactions. A similar behavior was experienced by Del Bene et al. [25] for the weak interactions with the B3LYP functional. The inclusion of the exact exchange into the functional (B3P or B3LYP methods) improves the agreement between the DFT and MP2 or composite results (see Table 1) considerably. Most of the energy calculations were performed with the MP2/cc-pVDZ geometries, because the geometry optimizations are rather expensive. The energetic effect of the geometry optimization was studied for the BP/6-31 + G(d) and the B3LYP/6-31 + G(d) calculations. The agreement with the best composite energy is slightly improved in the former and slightly worsened in the latter case by the geometry optimization. The relative energy changes are below 1.5 kcal/mol (see Table 1).

The reproduction of the correct energetic order for the two $^4C_1$ hydroxymethyl rotamers (**1** and **2**) is also a challenging task for the various methods. According to the experimental results the T rotamer

is less stable than the G + rotamer. The HF and MP2 methods are able to reproduce this energetic order only with the largest basis sets (see Table 1). The HF, MP2 or CCSD methods supplemented with polarized double-zeta quality basis sets provide the opposite energetic order than the experiment by 0.15–0.50 kcal/mol (see Table 1). Our recent GGA-DFT/6-31G(d) calculations provided even larger (0.7–0.8 kcal/mol) relative stabilization for the T rotamer compared to the G + rotamer [12]. Only the B3P/aug-cc-PVDZ//MP2/cc-pVDZ calculations indicated the G + rotamer (**1**) to be slightly more stable than the T rotamer (**2**).

3.2. Molecular geometry

For the G − g + hydroxymethyl rotamer of $^4C_1$β-D-glucose, (**1**), the experimental X-ray crystal structure is available [26]. The MP2/cc-pVDZ calculated geometry is in good agreement with the experimental results for the bond lengths [10]. The largest deviation is 0.01 Å (see Table 2). The endocyclic torsional angle differences between the calculated and experimental geometry range up to 5°, these variations, however, can be attributed to crystal packing effects [27]. Experimental data are not available for the other three conformers. For these conformers we take the MP2/cc-pVDZ calculated geometries as reference.

The results in Table 2 show that the bond lengthening correlation effects are largest in the BP/6-31G(d) method. Adding diffuse functions to the heavy atoms provide a further small bond lengthening (about 0.002 Å). The BP method clearly overcorrelates compared to the MP2 method in this sense. The introduction of the exact exchange in the hybrid forms of B3P or B3LYP decreases the bond lengthening effects. The results in Table 2 suggest the following relations for the C–C and C–O bond lengths: r(HF) < r(B3P) < r(MP2) < r(B3LYP) < r(BP) (all methods are supplemented with 6-31G(d) or 6-31 + G(d) basis sets). This observation is in perfect agreement with our earlier observations for C–O and O–H bond lengths with double- and triple-zeta quality basis sets [28]. The difference between the B3P, MP2 and B3LYP results is small (Table 2). It should be noted that for the bond angles the BP method shows a better agreement with the MP2 results than the hybrid methods (Table 2). The grid size influences the calculated molecular geometries only marginally (see Tables 2 and 3). This makes it possible to use the more economical sg1 grid instead of the more expensive fine grid for sugar calculations. The B3LYP/6-31 + G(d) calculations differ considerably from the MP2 and other calculations for $^1C_4$ conformer (**4**). The MP2 results show that the hexapyranose ring in this conformer is distorted by the O5 · · · H2–O2 · · · H4 and O1 · · · H3–O3 · · · H6–O6 · · · H1 interactions. In the B3LYP/6-31 + G(d) equilibrium geometry the C3–C2–O–H and C4–C3–O–H dihedral angles rotate from their starting positions (g + + and g − −, respectively) toward t positions (see Table 3 and Fig. 1), resulting in considerably smaller ring distortion and breaking the O1 · · · H3 and O5 · · · H2 interactions. Similar results were obtained by the BP/6-31 + G(d) calculations for the C3–C2–O–H dihedral angle (Table 3).

Table 3 shows the method and conformer dependence of the main geometric components of the O · · · H interactions. The difference between the ideal and calculated C–C–OH dihedral angles may signal the strength of the interaction. For the $^4C_1$ conformers the HF method turns these dihedral angles toward their ideal values, while the inclusion of electron correlation provides a larger difference from the ideal values (see Table 3 and Ref. [12]). For $^1C_4$ conformers, (**3**) and (**4**), the deviations of the C–C–O–H dihedral angles are as large as 40° and 55°, respectively. In these conformers the repulsive eclipsing interactions of the OH groups with the ring C–C bonds is counterbalanced by the O · · · H interactions and nearly eclipsed rotamers occur. However, this effect is rather sensitive to the method and basis set. For conformer (**4**) the inclusion of diffuse functions into the basis set turns the second and third OH groups away from the O4 and O1 atoms (see B3LYP or BP method in Table 3), respectively. This not only decreases the repulsive eclipsing interactions, but it also decreases the distortion of the ring as noted above. It is probable that larger basis sets would also influence the MP2 results of Barrows et al. [10]. Conformer (**3**) shows a fair stability in this respect. It should be noted that the H–C(n)–O–H dihedral angles, measurable by NMR experiments, can be derived within 3° error bar from the C(n +

Table 2
Comparison of geometrical parameters of the four selected β-D-glucose conformers for X-ray crystal, MP2, DFT and HF structure

	(1) $^4C_1$ ttttG + g −						(2) $^4C_1$ tttTg +						
	X-ray [b]	MP2 [c]	B3LYP	B3LYP /+	BP /+	HF	MP2 [c]	B3LYP	B3LYP /f	B3LYP /+	BP /+	HF	HF /+
bond lengths													
C1–C2	1.525	1.523	0.004	0.008	0.014	−0.004	1.523	0.005	0.006	0.007	0.013	−0.004	−0.002
C2–C3	1.520	1.517	0.005	0.007	0.012	0.000	1.517	0.006	0.006	0.008	0.013	0.001	0.002
C3–C4	1.511	1.520	0.007	0.009	0.014	0.000	1.518	0.005	0.006	0.007	0.011	0.000	0.001
C4–C5	1.529	1.526	0.007	0.009	0.014	−0.001	1.531	0.007	0.007	0.007	0.013	−0.002	−0.002
C5–C6	1.513	1.520	0.004	0.005	0.010	−0.002	1.527	0.005	0.005	0.005	0.011	−0.003	−0.002
O5–C1	1.433	1.422	0.002	0.001	0.015	−0.027	1.420	0.001	0.001	0.003	0.017	−0.026	−0.026
C1–O1	1.383	1.394	0.001	0.003	0.011	−0.017	1.394	0.002	0.002	0.004	0.012	−0.017	−0.016
C2–O2	1.429	1.420	0.002	0.005	0.015	−0.020	1.420	0.002	0.001	0.005	0.015	−0.020	−0.019
C3–O3	1.432	1.421	0.001	0.005	0.015	−0.020	1.421	0.001	0.001	0.004	0.015	−0.020	−0.020
C4–O4	1.419	1.418	0.000	0.004	0.014	−0.021	1.425	0.001	0.001	0.004	0.014	−0.023	−0.022
C5–O5	1.437	1.437	0.001	0.002	0.013	−0.022	1.430	0.002	0.002	0.005	0.015	−0.020	−0.020
C6–O6	1.419	1.416	0.001	0.006	0.015	−0.018	1.413	0.000	0.000	0.006	0.014	−0.019	−0.017
mean error			0.003	0.005	0.014	−0.013		0.003	0.003	0.005	0.014	−0.013	−0.012
valence angles													
C5–O5–C1	112.7	111.3	2.0	2.1	1.2	3.4	111.2	1.9	1.8	2.0	1.1	3.4	3.3
O5–C1–O1	107.0	109.3	−0.1	−0.3	−0.4	0.0	109.2	−0.2	0.2	−0.4	−0.5	0.0	−0.1
dihedral angles													
O5–C1–C2–C3	53.7	58.4	−1.3	−1.5	−1.0	−1.8	57.9	−1.0	−1.1	−1.4	−0.6	−2.0	−2.3
C1–C2–C3–C4	−50.8	−54.0	−0.1	0.5	0.3	0.4	−53.3	−0.4	−0.1	−0.2	−0.5	0.1	0.3
C2–C3–C4–C5	53.4	53.7	0.1	−0.2	0.0	−0.3	54.4	0.1	0.0	0.4	0.5	0.1	0.2
C3–C4–C5–O5	−59.8	−57.4	1.5	1.7	0.9	2.3	−58.7	1.8	1.5	1.3	1.0	1.8	1.4
C4–C5–O5–C1	66.3	63.5	−1.7	−1.5	−0.6	−1.8	64.0	−2.2	−1.8	−1.8	−1.5	−1.3	−1.1
C5–O5–C1–C2	−62.8	−63.9	1.5	1.1	0.4	1.2	−64.3	1.6	1.4	1.7	1.1	1.5	1.6
mean absolute error			1.0	1.1	0.6	1.3		1.2	1.0	1.1	0.9	1.1	1.1

	(3) $^1C_4$ tg+g−−g−G+g+						(4) $^1C_4$ g−−g++g−−g++G−g−			
	MP2 [c]	B3LYP	B3LYP /f	B3LYP /+	BP	BP /+	MP2 [c]	B3LYP	B3LYP /+	BP
bond lengths										
C1–C2	1.531	0.006	0.006	0.006	0.014	0.014	1.532	0.005	0.015	0.013
C2–C3	1.541	0.005	0.005	0.004	0.011	0.010	1.536	0.004	0.004	0.010
C3–C4	1.544	0.006	0.006	0.006	0.014	0.014	1.539	0.003	0.002	0.010
C4–C5	1.533	0.006	0.006	0.007	0.010	0.011	1.549	0.005	−0.001	0.011
C5–C6	1.549	0.008	0.007	0.008	0.015	0.017	1.528	0.004	0.009	0.009
O5–C1	1.422	0.000	0.000	0.003	0.015	0.010	1.419	−0.003	−0.005	0.010
C1–O1	1.419	0.003	0.003	0.007	0.015	0.019	1.410	0.004	−0.007	0.014
C2–O2	1.413	0.000	0.000	0.004	0.008	0.013	1.432	0.003	0.004	0.014
C3–O3	1.419	0.000	0.000	0.004	0.008	0.012	1.432	0.002	0.004	0.014
C4–O4	1.435	0.001	0.002	0.005	0.012	0.015	1.421	0.001	0.001	0.008
C5–O5	1.433	0.000	0.001	0.000	0.012	0.012	1.454	0.002	−0.012	0.015
C6–O6	1.427	0.001	0.001	0.001	0.014	0.013	1.426	0.001	0.002	0.011
mean error		0.003	0.003	0.005	0.012	0.013		0.003	0.001	0.012
valence angles										
C5–O5–C1	115.2	1.8	1.7	2.4	0.8	1.5	118.0	1.3	1.3	0.1
O5–C1–O1	112.2	−0.3	−0.3	−0.5	0.0	−0.2	115.6	−0.4	−0.9	−0.1
dihedral angles										
O5–C1–C2–C3	−57.8	1.2	1.2	2.2	−0.4	0.7	−62.3	1.7	13.4	−0.2
C1–C2–C3–C4	53.4	0.5	0.2	−1.0	1.7	0.4	59.6	−0.6	−11.2	0.5
C2–C3–C4–C5	−49.6	0.0	−0.1	1.5	−0.6	0.6	−47.3	−0.1	0.3	−0.7
C3–C4–C5–O5	48.2	−2.0	−1.5	−3.4	−1.6	−2.9	38.4	−0.6	7.6	0.2
C4–C5–O5–C1	−53.0	2.7	2.1	3.6	2.8	3.7	−43.1	1.0	−5.8	−0.2
C5–O5–C1–C2	58.5	−2.3	−2.0	−2.9	−1.9	−2.6	54.1	−1.2	−4.3	0.3
Mean absolute error		1.4	1.2	2.4	1.5	1.8		0.9	7.1	0.4

[a] The angles are in deg, the distances are in Å. The first column for a conformer shows the value of the geometric parameter, the following columns contain the difference. /f denotes fine grid, /+ denotes diffuse function added to the basis set.

[b] Ref. [26].

[c] Ref. [10].

Table 3
Geometrical parameters of the four selected β-D-glucose conformations calculated by MP2, HF and different GGA-DFT methods supplemented with 6-31G(d) or 6-31+G(d) basis sets [a]

		(1) $^4C_1$ ttttG+g−						(2) $^4C_1$ ttttTg+						
		MP2 [b]	B3LYP	B3LYP /+	BP /+	HF		MP2 [b]	B3LYP	B3LYP /f	B3LYP /+	BP /+	HF	HF /+
C2–C1–O–H	1	171.3	2.2	2.8	−0.4	6.6	1	174.9	3.2	3.0	4.2	1.3	7.0	8.3
C3–C2–O–H	2	179.1	1.1	3.2	2.8	3.4	2	178.8	0.9	0.7	3.0	2.3	3.8	5.2
C4–C3–O–H	3	183.3	−0.7	−2.5	−2.5	−2.0	3	183.6	0.6	0.5	−1.3	−0.7	−1.7	−2.9
C5–C4–O–H	4	169.7	0.5	2.0	0.6	4.0	4	172.1	0.6	0.4	0.7	0.9	1.2	1.2
O–C5–C6–O	5	58.8	−0.4	1.2	0.6	0.5	5	168.2	0.4	0.8	−1.6	−0.8	−1.5	−2.9
C5–C6–O–H	6	−52.4	−0.2	−4.4	−2.0	−6.0	6	50.6	0.5	0.3	1.1	0.6	2.9	2.8
$Ox\cdots Hy$	1···2						1···2							
O···H		2.446	0.055	0.106	0.106	0.077		2.448	0.049	0.047	0.100	0.093	0.083	0.112
C–O···H		78.5	−0.6	−0.6	−0.6	−0.8		78.5	−0.5	−0.5	−0.7	−0.4	−1.0	−1.1
R–O–C···H		140.6	1.7	2.5	−0.6	6.6		143.9	3.0	2.7	4.0	1.2	7.0	8.4
$Ox\cdots Hy$	2···3						2···3							
O···H		2.430	0.024	0.062	0.056	0.051		2.451	0.010	0.013	0.051	0.041	0.042	0.066
C–O···H		77.5	0.1	0.2	0.4	−0.3		77.1	0.2	0.1	0.3	0.5	−0.1	−0.1
R–O–C···H		−148.8	1.2	3.3	2.8	3.3		−148.8	1.0	0.9	3.0	2.3	3.6	4.9
$Ox\cdots Hy$	3···4						3···4							
O···H		2.360	0.014	0.052	0.033	0.063		2.346	0.024	0.020	0.054	0.048	0.052	0.070
C–O···H		76.9	0.3	0.5	0.6	0.2		78.1	0.2	0.2	0.3	0.5	−0.1	−0.1
R–O–C···H		149.2	−0.6	−2.4	−2.6	−1.3		150.7	0.7	0.5	−1.3	−0.6	−1.4	−2.7
$Ox\cdots Hy$	5···6						4···6							
O···H		2.261	0.033	0.128	0.084	0.116		1.970	0.047	0.038	0.090	0.050	0.148	0.169
C–O···H		80.3	0.2	−0.3	0.1	−0.2		100.5	−0.3	−0.3	0.9	0.8	0.1	0.9
R–O–C···H		−144.0	−1.3	−2.1	−0.8	−3.2		−157.5	2.5	2.2	0.3	1.2	1.9	−0.1

		(3) $^1C_4$ tg+g−−g−G+g+								(4) $^1C_4$ g−−g++g−−g++G−g−					
		MP2 [b]	B3LYP	B3LYP /f	B3LYP /+	BP /+	BP	HF		MP2 [b]	B3LYP	B3LYP /+	BP /+	BP	HF
C2–C1–O–H	1	−151.3	3.8	3.0	−0.7	4.2	7.2	−8.4	1	−107.4	−3.6	15.9	1.8	−0.7	−9.1
C3–C2–O–H	2	43.8	−0.7	−0.5	−1.7	−2.3	−1.9	1.7	2	104.1	0.9	66.5	55.3	−1.7	73.7
C4–C3–O–H	3	−93.3	−1.4	−1.6	−1.0	0.3	−0.6	−3.8	3	−115.2	−0.2	−51.3	−10.6	2.1	−14.0
C5–C4–O–H	4	−52.9	−1.7	−0.6	−4.3	−1.6	1.8	−9.2	4	90.1	2.5	−11.5	−10.2	0.9	−13.9
O–C5–C6–O	5	23.9	−3.2	−2.0	−1.9	−5.1	−4.8	89.1	5	−68.0	0.8	2.5	0.8	−0.5	4.7
C5–C6–O–H	6	41.9	0.4	−0.4	6.1	3.1	−5.8	6.6	6	−53.8	−0.1	−2.0	1.0	2.9	−6.6
O*x*···H*y*	1···3								1···3						
O···H		1.875	0.020	0.030	0.070	−0.003	−0.039	0.166		1.937	0.006		0.242	−0.065	0.294
C–O···H		99.8	−0.4	−0.4	0.3	0.0	−0.6	−0.4		96.3	0.7		−0.9	0.4	−0.6
R–O–C···H		−122.6	4.8	3.7	−0.2	5.4	8.2	−8.7		−84.6	−3.1		1.7	−1.0	−6.9
O*x*···H*y*	4···2								2···4						
O···H		1.937	0.033	0.033	0.092	0.038	−0.017	0.137		1.949	0.038	0.080	0.007	−0.011	0.094
C–O···H		97.5	0.0	0.3	0.1	−0.1	−0.5	0.4		99.8	−0.4	−0.5	1.2	−0.6	1.9
R–O–C···H		−132.2	−1.9	−1.1	−5.3	−1.8	2.3	−10.6		86.2	0.8	46.2	40.5	−0.4	58.7
O*x*···H*y*									3···6						
O···H										1.933	0.013	−0.073	−0.064	−0.056	0.133
C–O···H										108.4	0.6	5.0	1.6	−0.5	4.8
R–O–C···H										−89.7	−0.3	−39.0	−8.0	0.8	−10.7
O*x*···H*y*									5···2						
O···H										2.226	0.082			0.005	
C–O···H										72.8	−1.0			0.5	
R–O–C···H										97.2	−0.1			0.1	
O*x*···H*y*	6···1								6···1						
O···H		1.901	−0.002	0.007	0.119	−0.008	−0.090	0.291		1.7228	0.047	0.052	0.027	−0.013	0.211
C–O···H		92.8	2.3	1.7	2.2	3.0	2.1	−1.2		102.8	0.4	1.7	0.1	−0.2	1.3
R–O–C···H		107.2	−2.2	−2.1	3.1	−0.7	−7.6	7.9		−96.0	−1.3	−1.5	0.5	1.1	−5.4

[a] The angles are in deg, the distances are in Å. The first column for a conformer shows the value of the geometric parameter, the following columns contain the difference. /f denotes fine grid, /+ denotes diffuse functions added to the basis set.

[b] Ref. [10].

1)–C(n)–O–H dihedral angles by subtracting 120° (if $n = 1, 3$) or adding 120° (if $n = 2, 4$) to them at the HF and GGA-DFT levels of theory [12].

Some of the earlier characterizations of the O · · · H interactions used the O · · · H distance and one angle (e.g. O · · · H–O or R–O–C · · · H out of plane angle [29]). The O · · · H–O angle is not discussed here, because the linearity and non-linearity of the O · · · H–O angle is extensively discussed in the literature [30] and this parameter is completely insensitive to the spatial arrangement of the oxygen lone pairs. Also in sugars this angle is determined by other geometrical constraints and it deviates considerably from 180°. The low experimental IR frequencies for the proton acceptor bending signal that the energy hypersurface is flat in this direction and little energy is required to reorient the acceptor molecule [30]. The O · · · O distance and two angles are used for the precise description of symmetric, C_s, water dimer [31] or methanol and sylanol dimers [32].

Alternatively, the O · · · H interactions for non-symmetric cases can be characterized in a polar coordinate system centered on the O atom by three coordinates that provide the exact position of the H atom: the O · · · H distance, the C–O · · · H angle and the R–O–C · · · H dihedral angle.

Bader et al. have shown that two minima exist for the Laplace concentrations of electron density around the O atoms [33]. These minima are rigorous and exact mathematical representations of the O lone pairs. The position of these minima can be characterized the same way as the position of the H atoms (the sign of the dihedral angle tells at which side of the molecule the points are). The angular position of the points where the negative Laplacian attains its minimal value (LM) are 99–100° and ±104–105° for the C–O–LM and R–O–C · · · LM angles, respectively. Marshall et al. [34] considered these points as a site of electrophilic attack by the H atoms. Analysis of the 3D isosurfaces of the norm of the electron density gradient shows that an elliptic lens-shaped surface appears around the bond critical point between the interacting O an H [35]. Analysis of the 3D isosurfaces of the negative Laplacian concentration around the minima shows that the negative Laplacian concentration remains considerably large between the two minima (large torsion angles) and a sharp cut-off experienced at small angles (below 90°). Our investigation of the O · · · H interactions in 1,2-ethanediol also shows that the interaction is spatially extended [28]. A detailed discussion of the shape of the Laplacian concentration is beyond the scope of this Letter and will be given in a subsequent paper.

The results in Table 3 show that the various O · · · H interactions can readily be differentiated by the proposed geometric parameters. In the $^4C_1$ conformers the O · · · H distances, C–O · · · H bond angles and R–O–C · · · H torsion angles are in the range 2.26–2.45 Å, 77–80° and ±140–150°, respectively (Table 3). The geometric parameters of the O4 · · · H6 interaction in conformer (**2**) are different from these values (Table 3). For $^1C_4$ conformers the O · · · H distances are considerably smaller (1.72–1.95 Å) signalling a stronger interaction. The only exception is the O5 · · · H2 interaction in conformer (**4**) (Table 3). For $^1C_4$ conformers the C–O · · · H angles are closer to their optimal values and this gives a considerable stability for conformer (**3**), in which the dihedral angles are also close to their optimal values. In conformer (**4**) the O1 · · · H3 and O5 · · · H2 interactions are particularly weak. This can be attributed to the small C–O · · · H and/or R–O–C · · · H angles. The small angles for C–O · · · H or R–O–C · · · H provide weaker interaction while large R–O–C · · · H torsion angles (above 120°) are not so disadvantageous. This supports our proposition that the shape of the negative Laplacian concentration around the O atom plays a role in the interaction.

5. Conclusions

The following conclusions can be drawn from the discussion above.

(1) GGA- or hybrid-DFT methods and the MP2 method provide similar energetic differences for β-D-glucose conformers. Addition of the diffuse functions to a double-zeta quality basis set and inclusion of the exact exchange into the DFT functionals improve the agreement between the DFT and MP2 or best composite estimates of the energetic differences considerably.

(2) The GGA- or hybrid-DFT results show that these methods reproduce the geometrical conse-

quences of correlation effects correctly for glucose. The extent of the correlation effects, however, varies with the applied functional. For C–C and C–O bond lengths the order is the following: $r(\mathrm{HF}) < r(\mathrm{B3P}) < r(\mathrm{MP2}) < r(\mathrm{B3LYP}) < r(\mathrm{BP})$. The BP method shows the best agreement with the MP2 results for the bond angles.

(3) The difference between the ideal and calculated C–C–OH dihedral angles signals the strength of the O · · · H interactions. The inclusion of the electron correlation provides larger differences for the $^4C_1$ conformers. For the $^1C_4$ conformers the deviations are large because the repulsive eclipsing interactions of the OH groups with the ring C–C bonds is counterbalanced by the O · · · H interactions and nearly eclipsed rotamers occur. However, this effect is rather sensitive to the method and basis set. The inclusion of the diffuse functions into the basis set results in different rotamers.

(4) We characterized O · · · H interactions in a polar coordinate system centered on the O atom by three (one radial and two angular) coordinates. The analysis shows that the angular position of the minima of the negative Laplacian concentrations (LM) are 99–100° and ±104–105° for the C–O–LM and R–O–C · · · LM angles, respectively. Our results indicate that the various O · · · H interactions can readily be differentiated by the proposed geometric parameters. The small values for angular coordinates provide weaker interactions while large R–O–C · · · H torsion angles (above 120°) are not so disadvantageous in this respect. This supports that the shape of the negative Laplacian concentration around the O atom plays a role in the interaction.

Acknowledgement

The authors are grateful to Alfred D. French for the MP2/cc-pDVZ coordinates and for a preprint of Ref. [10]. The financial support of the Hungarian Research Foundation (OTKA T14975, and T16328) is acknowledged. The continuous financial support of the Natural Sciences and Engineering Research Council (NSERC) is gratefully acknowledged.

References

[1] J.W. Brady, J. Am. Chem. Soc. 111 (1989) 5155.
[2] B.P. van Eijck, L.M.J. Kroon-Batenburg and J. Kroon, J. Mol. Struct. 237 (1990) 315.
[3] S. Ha, J. Gao, B. Tidor, J.W. Brady and M. Karplus, J. Am. Chem. Soc. 113 (1991) 553.
[4] P.L. Polavarapu and C.S. Ewig, J. Comput. Chem. 13 (1992) 1255.
[5] R.G. Zhbankov, J. Mol. Struct. 275 (1992) 645.
[6] C.J. Cramer and D.G. Truhlar, J. Am. Chem. Soc. 115 (1993) 5745.
[7] B.P. van Eijck, R.W.W. Hooft and J. Kroon, J. Phys. Chem. 97 (1993) 12093.
[8] U. Salzner and P.v.R. Schleyer, J. Org. Chem. 59 (1994) 2138.
[9] T.M. Glennon, Y.J. Zheng, S.M. Legrand, B.A. Shutzberg, and K.M. Merz Jr, J. Comput. Chem. 15 (1994) 1019.
[10] S.E. Barrows, F.J. Dulles, C.J. Cramer, A.D. French and D.G. Truhlar, Carbohydr. Res. 276 (1995) 219.
[11] M.K. Dowd, A.D. French and P.J. Reilley, Carbohydr. Res. 264 (1994) 1.
[12] G.I. Csonka, I. Kolossváry, P. Császár, K. Éliás and I.G. Csizmadia, J. Mol. Struct. accepted.
[13] Y. Nishida, H. Ohrui and H. Meguro, Tetrahedron Letters 25 (1984) 1575.
[14] G.M. Brown and H.A. Levy, Acta Crystallogr. Sect. B (1979) 656.
[15] A.D. Becke, Phys. Rev. A 38 (1988) 3098.
[16] J.P. Perdew, Phys. Rev. B 33 (1986) 8822.
[17] S.H. Vosko, L. Wilk and M. Nusair, Can. J. Phys. 58 (1980) 1200.
[18] A.D. Becke, J. Chem. Phys. 98 (1993) 5648.
[19] M.J. Frisch, G.W. Trucks, M. Head-Gordon, P.M.W. Gill, M.W. Wong, J.B. Foresman, B.G. Johnson, H.B. Schlegel, M.A. Robb, E.S. Replogle, R. Gomperts, J.L. Andres, K. Raghavachari, J.S. Binkley, C. Gonzalez, R.L. Martin, D.J. Fox, D.J. DeFrees, J. Baker, J.J.P. Stewart and J.A. Pople, GAUSSIAN 92/DFT, Revision G (Gaussian, Inc., Pittsburgh, PA, 1993).
[20] C. Lee, W Yang and R.G. Parr, Phys. Rev. B 37 (1988) 785.
[21] M.J. Frisch, G.W. Trucks, M. Head-Gordon, P.M.W. Gill, M.W. Wong, J.B. Foresman, B.G. Johnson, H.B. Schlegel, M.A. Robb, E.S. Replogle, R. Gomperts, J.L. Andres, K. Raghavachari, J.S. Binkley, C. Gonzalez, R.L. Martin, D.J. Fox, D.J. DeFrees, J. Baker, J.J.P. Stewart and J.A. Pople, GAUSSIAN 94, Revision B (Gaussian, Inc., Pittsburgh, PA, 1995).
[22] W.J. Hehre, L. Radom, P.v.R. Schleyer and J.A. Pople, Ab initio molecular orbital theory (Wiley, New York, 1986) and references cited therein.
[23] T.H. Dunning, J. Chem. Phys. 90 (1989) 1007.
[24] P.M.W. Gill, B.G. Johnson and J.A. Pople, Chem. Phys. Letters 217 (1994) 65.

[25] J.E. Del Bene, W.B. Person and K. Szczepaniak, J. Chem. Phys. 99 (1995) 10705.
[26] S.S.C. Chu and G.A. Jeffrey, Acta Crystallogr. B 24 (1968) 830.
[27] A.D. French, R.S. Rowland and N.L. Allinger, in: Computer modeling of carbohydrate molecules, ACS Symposium Series 430, eds. A.D. French and J.W. Brady (American Chemical Society, Washington, DC, 1990) p. 120.
[28] G.I. Csonka and I.G. Csizmadia, Chem. Phys. Letters 243 (1995) 419.
[29] L. Van den Enden, C. Van Alsenoy, J.N. Scarsdale and L. Shäfer, J. Mol. Struct. THEOCHEM 104 (1983) 471.
[30] S. Sheiner, in: Reviews in computational chemistry, Vol II eds. K.B. Lipkowitz and D.B. Boyd (VCH, New York, 1991) p. 165 and references cited therein.
[31] M.J. Frisch, J.E. Del Bene, J.S. Binkley and H.F. Schaefer III, J. Chem. Phys. 84 (1986) 2279.
[32] A. Bleiber and J. Sauer, Chem. Phys. Letters 238 (1995) 243.
[33] R.F.W. Bader, P.J. MacDougall and C.D.H. Lau, J. Am. Chem. Soc. 106 (1984) 1594.
[34] M.T. Carrol, C. Ghang and R.F.W. Bader, Mol. Phys. 63 (1988) 387.
[35] G.I. Csonka, N. Anh, J. Ángyán and I.G. Csizmadia, Chem. Phys. Letters 245 (1995) 129.